PHILOSOPHICAL TRANSACTIONS OF THE ROYAL SOCIETY A MATHEMATICAL, PHYSICAL & ENGINEERING SCIENCES

Chaos from a Hysteresis and Switched Circuit

Toshimichi Saito and Shinji Nakagawa

Phil. Trans. R. Soc. Lond. A 1995 **353**, 47-57
doi: 10.1098/rsta.1995.0089

Chaos from a hysteresis and switched circuit

By Toshimichi Saito and Shinji Nakagawa

EE Dept, HOSEI University, Tokyo 184, Japan

This paper considers a simple piecewise linear hysteresis circuit. We define one-dimensional return map and derive its analytic formula. It enables us to give a sufficient condition for chaos generation and to analyse bifurcation phenomena rigorously. Especially, we have discovered period-doubling bifurcation with symmetry breaking. Some of theoretical results are verified by laboratory measurements.

1. Introduction

Analysis of chaos and related bifurcations is an important nonlinear problem (see Ott 1993 and references therein). In the analysis, piecewise linear (PWL) circuits are useful tools because both theoretical and laboratory approaches are relatively easy. There are interesting results on three-dimensional PWL autonomous chaotic circuits, e.g. the analysis of Shil'nikov's chaos and related bifurcation (Chua *et al.* 1986; Chua *et al.* 1993). Also, control and synchronization of chaos are hot topics for engineering applications of chaos (Ott *et al.* 1990; Ogorzałek 1993; Pecora *et al.* 1990; Hasler *et al.* 1993). Chaos seems to play an important role for efficient information processor, communication system and so on.

This paper considers chaos and fundamental bifurcations from a simple PWL hysteresis and switched circuit. Basically, the circuit dynamics are described by a three-dimensional constrained equation (Saito 1985) and in an idealized case, it is described by two linear two-dimensional equations connected to each other by hysteresis switchings. Then we define one-dimensional return map and give its analytic formula. Using this return map, we can give a sufficient condition for chaos generation, where chaos is characterized by ergodicity (Li *et al.* 1978) and positive Lyapunov exponent. Rigorous proof of chaos generation in this sense is hard for usual three-dimensional autonomous systems. In the phase space, chaotic attractor exhibits single or double-screw form. We also analyse fundamental bifurcation phenomena for periodic window that is usually born via tangent bifurcation and is to be chaotic via period-doubling cascade. Then it disappears via crisis (Ott 1993). Using an analytic equation, we give parameter sets for tangent bifurcation, period-doubling bifurcation and crisis. Especially, the first period doubling in the return map corresponds to symmetry breaking of attractor in the phase space. It changes the number of attractors from one to two. Moreover, complicated domain of attraction and classification of chaos are considered. Some of theoretical results are verified by laboratory experiments. We have published some works on hysteresis chaos generators (Newcomb *et al.* 1984; Saito 1984, 1990; Saito *et al.* 1994; Suzuki *et al.* 1994) and this paper provides a developed version of the three-dimensional case.

Phil. Trans. R. Soc. Lond. A (1995) **353**, 47–57
Printed in Great Britain

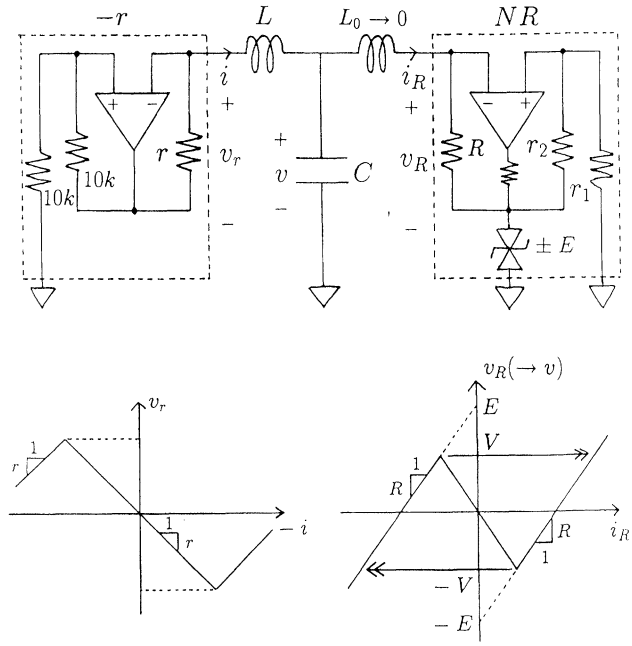

Figure 1. Hysteresis chaos generator.

2. Circuit and return map

Figure 1 shows the chaos generator. In this figure, the left op amp realizes a linear negative resistor characterized by $v_r = -r(-i)$. Basically, it is a three-segment current controlled resistor and we use only its central region. The right op amp realizes another current controlled resistor characterized by

$$v_R = \begin{cases} Ri_R + E, & \text{for} \quad i_R \leqslant -(E-V)/R, \\ -[RV/(E-V)]i_R, & \text{for} \quad |i_R| < (E-V)/R, \\ Ri_R - E, & \text{for} \quad i_R \geqslant (E-V)/R, \end{cases} \tag{1}$$

where E is the Zener voltage and $V \equiv r_1 E/(r_1 + r_2) < E$. If the small serial inductor L_0 is shorted, v_R approaches to v and the above characteristic is to be hysteresis:

$$i_R = \frac{1}{R}(v + H(v)), \quad H(v) = \begin{cases} E, & \text{for} \quad v \geqslant -V, \\ -E, & \text{for} \quad v \leqslant V, \end{cases} \tag{2}$$

where $H(v)$ is switched from E to $-E$ if v hits the threshold $-V$ and vice versa as shown in figure 2.

A theoretical evidence for such hysteresis behaviour is discussed in Saito (1990) and Kennedy *et al.* (1991). Using the hysteresis characteristic, the circuit dynamics are described by

$$RC\frac{\mathrm{d}}{\mathrm{d}t}v = Ri - (v + H(v)), \quad L\frac{\mathrm{d}}{\mathrm{d}t}i = -v + ri. \tag{3}$$

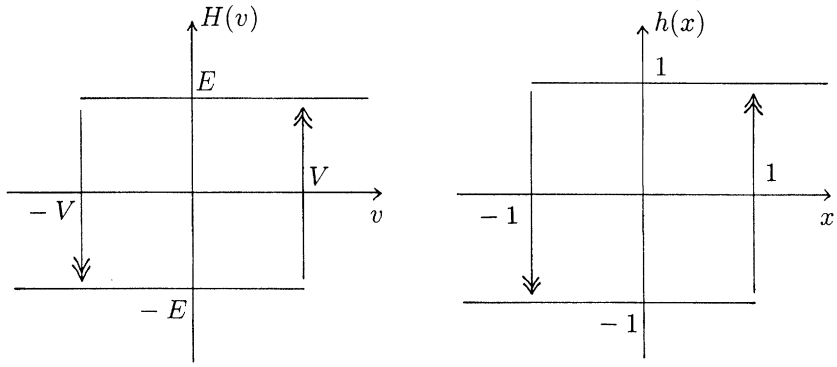

Figure 2. Hysteresis characteristic.

Moreover, using the following-dimensionless variables and parameters:

$$\tau' = \frac{t}{RC}, \quad x = \frac{v}{V}, \quad Y = \frac{Ri}{V}, \quad a = \frac{CR^2}{L}, \quad b = \frac{r}{R}, \quad c = \frac{E}{V}.$$

Equation (3) is transformed into

$$\frac{\mathrm{d}}{\mathrm{d}\tau'}\begin{bmatrix} x \\ Y \end{bmatrix} = \begin{bmatrix} -1 & 1 \\ -a & ab \end{bmatrix}\left[\begin{bmatrix} x \\ Y \end{bmatrix} - \begin{bmatrix} b \\ 1 \end{bmatrix}\frac{\mathrm{ch}(x)}{1-b}\right], \tag{4}$$

where $h(x)$ is a normalized hysteresis defined by $h(x) \equiv E^{-1}H(Vx)$. In this paper, we consider the case where the above coefficient matrix has unstable complex eigenvalues $\delta\omega \pm \mathrm{j}\omega$, $\delta > 0$, $\omega > 0$. Then applying the transformation,

$$\tau = \omega\tau', \quad y = -\frac{\delta\omega + 1}{\omega}x + \frac{1}{\omega}Y,$$

we can transform equation (4) into the following Jordan form:

$$\begin{bmatrix} \dot{x} \\ \dot{y} \end{bmatrix} = \begin{bmatrix} \delta & 1 \\ -1 & \delta \end{bmatrix}\left[\begin{bmatrix} x \\ y \end{bmatrix} - \begin{bmatrix} p \\ q \end{bmatrix} h(x)\right], \tag{5}$$

where $\dot{}$ denotes $\mathrm{d}/\mathrm{d}\tau$. This equation has three parameters (δ, p, q) and they are given by original three parameters (a, b, c):

$$\delta = \frac{ab-1}{2\omega}, \quad p = \frac{bc}{1-b}, \quad q = \frac{1}{2\omega}\left(2c - \frac{(ab-1)bc}{1-b}\right),$$

where $\omega^2 \equiv a(1-b) - \frac{1}{4}(ab-1) > 0$ and we assume $p \geqslant 0$. This equation can be regarded as two linear equations on two half-spaces connected to each other by the hysteresis switchings of h, where the half-spaces are

$$S_+ = \{(x, y, h) | x \geqslant -1, h = 1\}, \quad S_- = \{(x, y, h) | x \leqslant 1, h = -1\}. \tag{6}$$

S_+ and S_- correspond to the upper and the lower branches of $h(x)$, respectively. Note that this Jordan form governs a certain class of circuits that includes one symmetric hysteresis resistor (Saito 1990). Then the solution on S_+ is given by

$$\begin{bmatrix} x(\tau) - p \\ y(\tau) - q \end{bmatrix} = \mathrm{e}^{\delta\tau}\begin{bmatrix} \cos\tau & \sin\tau \\ -\sin\tau & \cos\tau \end{bmatrix}\begin{bmatrix} x(0) - p \\ y(0) - q \end{bmatrix}, \tag{7}$$

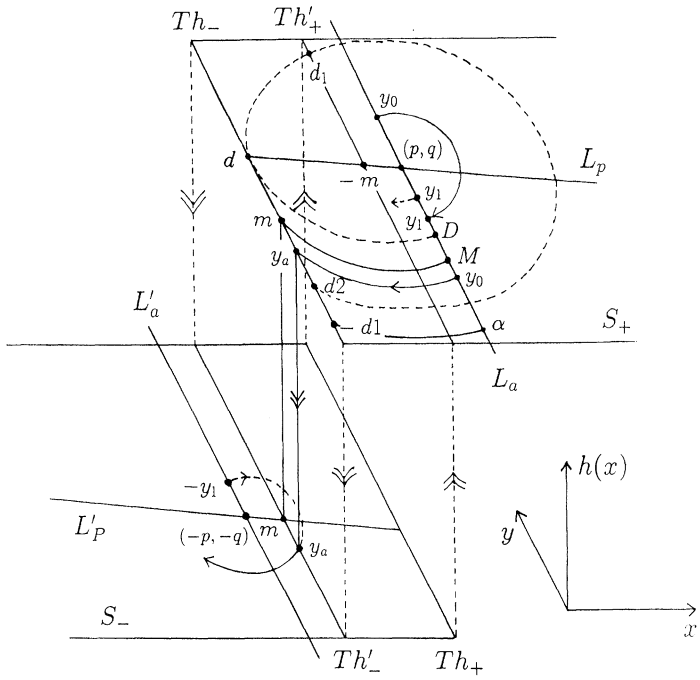

Figure 3. Hysteresis phase space.

for $0 < \tau < \tau_s$, where τ_s is switching time when x hits the threshold and jumps to S_-. Note that τ is identical with the clockwise angle from $(x(0)-p, y(0)-q)$ to $(x(\tau)-p, y(\tau)-q)$. The solution on S_- is symmetric to this.

To derive the return map, we define some objects as shown in figure 3. Let $Th_- = \{(x,y,h)|x = -1, h = 1\}$, $Th'_+ = \{(x,y,h)|x = 1, h = 1\}$, $L_a = \{(x,y,h)|x = p, h = 1\}$ and let Th_+, Th'_- and L'_a be symmetric to Th_-, Th'_+ and L_a, respectively. Th_- and Th_+ are the left and the right hysteresis thresholds, respectively. Then let points on these lines be represented by their y coordinate, e.g. $y \in L_a$ implies $(p,y,1) \in L_a$. Let $L_p = \{(x,y,h)|\delta(x-p)+(y-q) = 0, h = 1\}$, $d = Th_- \cap L_p$, $-m = Th'_+ \cap L_p$ and let m be symmetric to $-m$, where $\dot{x} = 0$ on L_p, $d = q+\delta(p+1)$ and $-m = q+\delta(p-1)$. Here, note that the trajectory starting from d passes through a point d_1 on Th'_+ and it hits a point d_2 on Th_-. On L_a, there exist three points D, M and α such that trajectories starting from them pass through three points d, $m \in Th_-$ and $-d_1 \in Th_-$, respectively. These points will play an important role for the return map. Note that $d_2 > -d_1$ guarantees that the trajectory starting from D dose not diverge.

After these preparations, we try to define the return map. First, letting $L_d = \{(x,y,h)|x = p, y > \alpha, h = 1\}$, we consider a trajectory starting from a point $y_0 \geqslant D$ on L_d at $\tau = 0$. It rotates divergently around the equilibrium $(p,q) \in S_+$ and intersects L_a at $\tau = \pi$. Let y_1 be the intersection. Next, we consider a trajectory starting from a point $y_0 < D$ on L_d at $\tau = 0$. This trajectory moves on S_+ and it hits a point y_a on Th_- and then it jumps to the same point y_a on Th'_-. Let τ_1 be the hit time. Here, we consider three cases: $p < 1$, $p = 1$ and $p > 1$. If $p < 1$ then L'_a is the right-hand side of Th'_- and the trajectory starting from y_a at $\tau = 0$ intersects L'_a at some positive time τ_2. Let $-y_1$ be the intersection on L'_a. If $p = 1$ then L'_a

is identical with Th'_- hence let $-y_1 \equiv y_a$. If $p > 1$ then L'_a is the left-hand side of Th'_-. In this case, we remark that there exists some point $-y_1 \in L'_a$ such that the trajectory starting from it at $\tau = 0$ passes through $y_a \in Th'_-$ at some positive time $\tau = \tau_3$. That is, we can find the following route for $y_0 < D$:

$$y_0 \in L_d \to y_a \in Th'_- \to -y_1 \in L'_a. \tag{8}$$

For the three cases of p, we note that the trajectory starting from $-y_1 \in L'_a$ at $\tau = 0$ is symmetric to the trajectory starting from $y_1 \in L_a$ at $\tau = 0$. Consequently, we can define one-dimensional return map F from L_d to L_a that transforms a point $y_0 \in L_d$ to a point $y_1 \in L_a$. Then we have

Theorem 1. *The return map can be formulated by*

$$F(y_0) = \begin{cases} F_1(y_0), & \text{for} \quad y_0 \geqslant D, \\ F_3 \circ F_2(y_0), & \text{for} \quad y_0 < D, \end{cases} \tag{9a}$$

where

$$y_1 = F_1(y_0) \equiv -\mathrm{e}^{\delta\pi}(y_0 - q) + q, \tag{9b}$$

$$y_0 = F_2^{-1}(y_a) = -\sqrt{[(y_a - q)^2 + (p+1)^2]}\mathrm{e}^{-\delta\tau_1} + q, \tag{9c}$$

$$y_1 = F_3(y_a) = \begin{cases} -\sqrt{[(y_a + q)^2 + (1-p)^2]}\mathrm{e}^{\delta\tau_2} + q, & \text{for} \quad p < 1, \\ -y_a, & \text{for} \quad p = 1, \\ -\sqrt{[(y_a + q)^2 + (p-1)^2]}\mathrm{e}^{-\delta\tau_3} + q, & \text{for} \quad p > 1, \end{cases} \tag{9d}$$

$$\tau_1(y_a) = \tfrac{1}{2}\pi - \arctan\frac{q - y_a}{p+1}, \tag{9e}$$

$$\tau_2(y_a) = \tfrac{1}{2}\pi - \arctan\frac{y_a + q}{1-p}, \tag{9f}$$

$$\tau_3(y_a) = \tfrac{1}{2}\pi - \arctan\frac{y_a + q}{p-1}. \tag{9g}$$

Proof. We show only for F_2^{-1}. Let the trajectory starting from $(p, y_0, 1) \in L_d$ hits point $(-1, y_a, 1) \in Th_-$ at $\tau = \tau_1$. Substituting

$$(\tau_1, p, y_0, -1, y_a) \quad \text{for} \quad (\tau, x(0), y(0), x(\tau), y(\tau))$$

in equation (7), we obtain

$$\begin{bmatrix} p - p \\ y_0 - q \end{bmatrix} = \mathrm{e}^{-\delta\tau_1} \begin{bmatrix} \cos\tau_1 & -\sin\tau_1 \\ \sin\tau_1 & \cos\tau_1 \end{bmatrix} \begin{bmatrix} -1 - p \\ y_a - q \end{bmatrix}. \tag{10}$$

Since τ_1 coincides with the clockwise angle from $(0, y_0 - q)$ to $(-1 - p, y_a - q)$, τ_1 is given by (9*e*). Also, the second row in equation (10) is equivalent to (9*c*). ■

Note that D and M are given by $F_2^{-1}(d)$ and $F_2^{-1}(m)$, respectively. We will use equation (9*c*) of F_2^{-1} to prove chaos generation. Also, we will use the following equation for numerical calculation of F_2:

$$\left.\begin{aligned} y_a &= (y_0 - q)\mathrm{e}^{\delta\tau_1}\cos\tau_1 + q, \\ f(y_0, \tau_1) &\equiv (y_0 - q)\mathrm{e}^{\delta\tau_1}\sin\tau_1 + 1 + p = 0, \end{aligned}\right\} \tag{11}$$

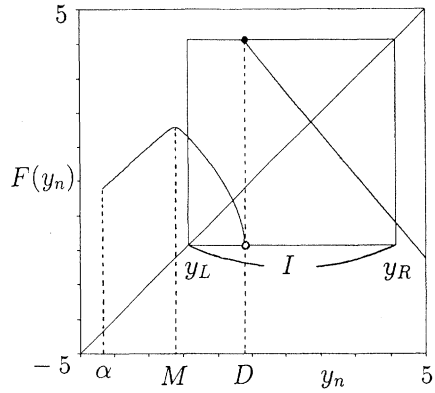

Figure 4. Return map for $(a = 5, b = 0.25, c = 3.5)$.

where f gives the hit time τ_1 for given y_0. f has unique solution in $(0, \frac{1}{2}\pi + \arctan\delta)$ and can be calculated by

$$\tau_1(n+1) = \tau_1(n) - f(y_0, \tau_1(n)) \left(\frac{\partial f}{\partial \tau}(y_0, \tau_1(n)) \right)^{-1},$$

where $\tau_1(0) = 2\arctan\delta$. Since f is concave on $(\tau_1(0), \pi + \tau_1(0))$ and is convex on $(\tau_1(0) - \pi, \tau_1(0))$, this Newton and Raphson iteration must converge to the unique solution. Next, differentiating (9*b*) to (9*d*) gives the following.

Theorem 2. *Derivative of the return map is given by*

$$DF(y) \equiv \frac{\mathrm{d}F}{\mathrm{d}y} = \begin{cases} -\mathrm{e}^{\delta\pi}, & \text{for} \quad y \geqslant D, \\ \dfrac{\mathrm{d}F_3}{\mathrm{d}y_a} \left(\dfrac{\mathrm{d}}{\mathrm{d}y_a} F_2^{-1} \right)^{-1}, & \text{for} \quad y < D, \end{cases} \tag{12}$$

where $y_a = F_2(y)$ *and*

$$\frac{\mathrm{d}}{\mathrm{d}y_a} F_2^{-1} = -\frac{y_a - d}{\sqrt{[(y_a - q)^2 + (p+1)^2}}]\mathrm{e}^{-\delta\tau_1},$$

$$\frac{\mathrm{d}F_3}{\mathrm{d}y_a} = \begin{cases} -\dfrac{y_a - m}{\sqrt{[(y_a + q)^2 + (p-1)^2]}} \mathrm{e}^{\delta\tau_2}, & \text{for} \quad p < 1, \\ 1 & \text{for} \quad p = 1, \\ -\dfrac{y_a - m}{\sqrt{[(y_a + q)^2 + (p-1)^2]}} \mathrm{e}^{-\delta\tau_3}, & \text{for} \quad p > 1. \end{cases}$$

Figure 4 shows an example of the return map. F is half-line for $y \geqslant D$, is concave for $y < D$ and $F(M) < q$ is local maximum. If we can iterate F, the dynamics is simplified into $y_{n+1} = F(y_n)$ and y_n coincides with the original trajectory for every twice hitting at $(\alpha, D) \in L_d$.

Figure 5 shows some examples of the return map and corresponding attractors. In this figure, we can see that the first period doubling in the return map causes symmetry breaking of the periodic attractor. Then the doubling cascade goes to asymmetric chaos as b decreases. Since equation (5) is symmetric, the symmetry breaking changes the number of attractor from one to two. Also, figure 6 shows

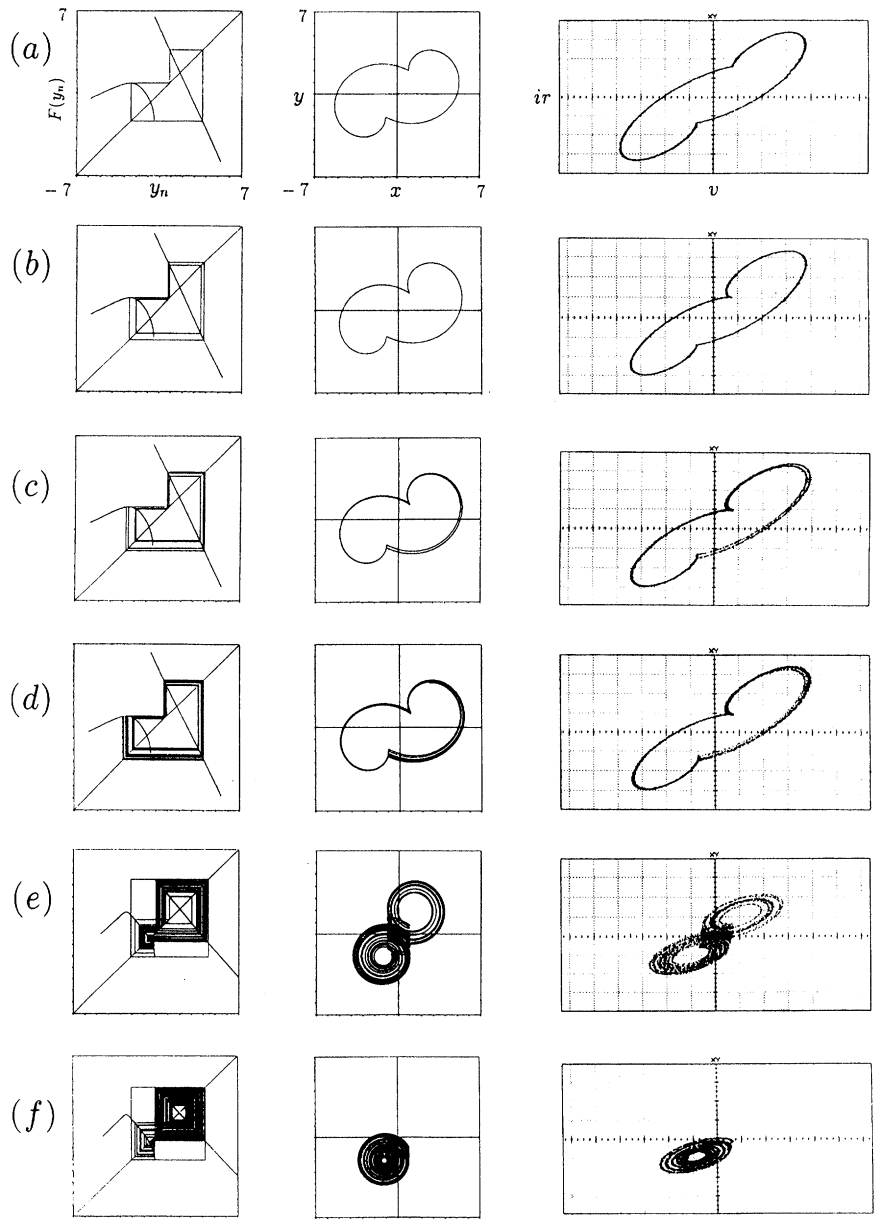

Figure 5. Typical attractors for $(a = 5, c = 4)$. $(L \doteq 200m,\ C \doteq 10n,\ R \doteq 10k,\ V \doteq 0.7,\ E \doteq 2.7)$. (a) 01^2-SPS for $b = 0.37$ $(r \doteq 4.25k)$. (b) $(01^2)^2$-SPS for $b = 0.363$ $(r \doteq 4.15k)$. (c) $(01^2)^4$-SPS for $b = 0.3613$ $(r \doteq 4.14k)$. (d) Chaos for $b = 0.36$ $(r \doteq 4.13k)$. (e) Double-screw chaos for $b = 0.24$ $(r \doteq 3.02k)$. (f) Single-screw chaos for $b = 0.22$ $(r \doteq 2.82k)$.

a one-parameter bifurcation diagram. The periodic attractors in figure 5 are in a periodic window in figure 6 and other similar periodic windows exist. For small b, such periodic window does not exist no longer and almost attractors are to be chaotic.

PHILOSOPHICAL TRANSACTIONS OF THE ROYAL SOCIETY A MATHEMATICAL, PHYSICAL & ENGINEERING SCIENCES

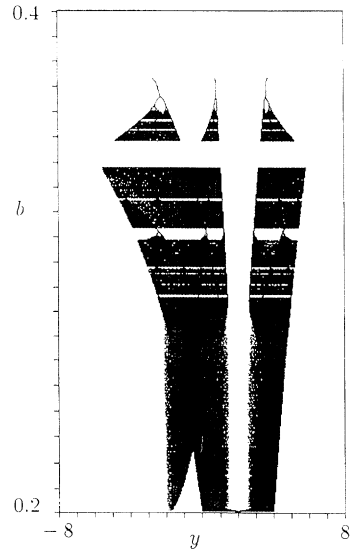

Figure 6. One-parameter bifurcation for $(a = 5, c = 4)$.

Then the symmetric double-screw chaos changes to asymmetric single-screw chaos as b decreases further. We analyse such phenomena in more detail.

3. Chaos and bifurcation

First, we define periodic point.

Definition 1. $y_q \in L_d$ is said to be a periodic point with period q if $y_q = F^q(y_q)$ and $y_q \neq F^k(y_q)$ for $0 < k < q$, where F^n denotes n times composite of F. A periodic point y_q is said to be stable periodic point (SPP) if $|DF^q(y_q)| < 1$. Especially, SPP with $|DF(y_q)| = 0$ is said to be superstable. Also, a sequence of SPP, $\{F(y_q), \ldots, F^q(y_q)\}$, is said to be stable periodic sequence (SPS). An SPS that includes M is superstable.

Here, note that an SPS that includes even number (respectively, odd number) of SPP in (α, D) implies existence of two asymmetric attractors (respectively, one symmetric attractor). Then we symbolize an SPS by applying the following for its SPP y_q:

$$\Omega(y_q) = \begin{cases} 0, & \text{for} \quad y_q < D, \\ 1, & \text{for} \quad y_q \geqslant D. \end{cases} \tag{13}$$

For example, SPSs in figure 5*a–c* are symbolized as (01^2), $(01^2)^2$ and $(01^2)^4$, respectively, where the power number implies the successive same symbol. Here, we consider fundamental SPS symbolized by 01^{2n} and refer to it as 01^{2n}-SPS. F exhibit (01^{2n})-SPS if there exits an SPP y_q such that

$$q > y_q > F^2(y_q) > \ldots > D > F^{2n}(y_q), \quad F^{2n+1}(y_q) = y_q, \quad |DF^{2n+1}(y_q)| < 1. \tag{14}$$

We can confirm this condition analytically by using equations (9) and (12). Especially, note that $DF^{2n+1}(y_q) = \mathrm{e}^{2n\delta\pi} DF(F^{2n}(y_q))$ is satisfied in (14). Then the period-doubling bifurcation set can be calculated by replacing the last inequality in (14) with $DF^{2n+1}(y_q) = -1$. Similar calculation is possible for the successive

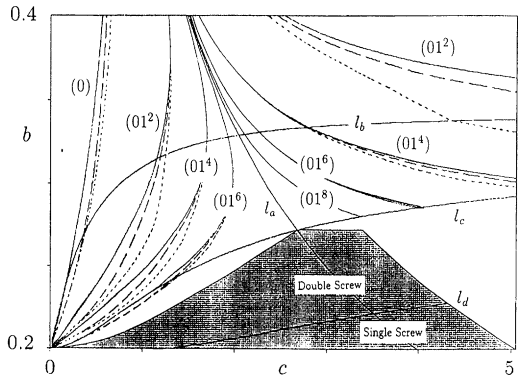

Figure 7. Bifurcation diagram for $a = 5$. Labelled dotted line, crisis set; labelled broken line, period-doubling bifurcation set; labelled solid line, tangent bifurcation set; l_a, $p = 1$; l_b, $F(y_L) = y_L$; l_c, $y_L = M$; l_d, $F^3(D) = F^2(D)$; and shaded region satisfies chaos generating condition.

period-doubling bifurcation sets. Also, the tangent bifurcation set can be calculated by replacing the last inequality in (14) with $DF^{2n+1}(y_q) = 1$.

As shown in figure 6, the SPS is born via tangent bifurcation and is to be chaotic via period-doubling cascade as b decreases. Then, after the tangent bifurcation, there exists one symmetric attractor and after the first period-doubling bifurcation, there exist two asymmetric attractors. In figure 7, the labelled solid and broken curves indicate parameter sets for tangent bifurcation and first period-doubling bifurcation, respectively. Also, F exhibits (01^{2n}) periodic window if condition (14) or following condition is satisfied:

$$\left.\begin{aligned} &F(M) > F^3(M) > \ldots > D > F^{2n+1}(M) > M, \\ &F^{2(2n+1)+1}(M) \geqslant F^{(2n+1)+1}(M) \geqslant F^{-2n+1}(y_d), \end{aligned}\right\} \tag{15}$$

$$y_d \equiv \begin{cases} D, & \text{for} \quad p \leqslant 1, \\ F^{-1}(y_{d'}), & \text{for} \quad p > 1, \end{cases}$$

where $y_{d'} \equiv \min(F(D), F^{-1}(\alpha))$ and F^- denote inverse of F. This (01^{2n}) periodic window disappears via crisis (see figure 6). Also, the crisis set can be calculated by replacing the second inequality in (15) with $F^{2(2n+1)+1}(M) = F^{(2n+1)+1}(M) \geqslant F^{-2n+1}(y_d)$ or $F^{2(2n+1)+1}(M) \geqslant F^{(2n+1)+1}(M) = F^{-2n+1}(y_d)$. In figure 7, the dotted curves indicate parameter set for crisis. Namely, we can observe (01^{2n}) periodic window between solid curve and dotted curve. Note that the bifurcation sets accumulate to the curve l_a on which $p = 1$ is held. Then we have the following:

Theorem 3. *Let $y_R \equiv F(D)$, y_L be the smaller one of $F(D_-)$ and $F^2(D)$ and let $I \equiv [y_L, y_R]$. $F(I) \subseteq I$ is satisfied if $F(y_L) > y_L$. We refer to I as an invariant interval of F.*

Proof. This theorem is derived directly from fundamental characteristics of the return map: $F(M)$ is the unique extremum for $y < D$, F is half-line for $y \geqslant D$ and $F(M) < q$. ■

In figure 7, $F(y_L) = y_L$ is satisfied on curve l_b and I is the invariant interval under this curve. And existence of bifurcation sets upper the curve l_b implies that domain

of attraction to the SPS is not simple: some initial value converges to the SPS and some initial value causes divergence (see figure 6). Then the following is basic to prove chaos generation.

Theorem 4. *$F(y)$ is exactly convex for $M < y < D$.*

Proof. We show only for $p > 1$. Letting $G(y) = \ln(-DF(y))$ for $M < y < D$ and differentiating it, we obtain

$$\frac{\mathrm{d}G}{\mathrm{d}y} = \left[\frac{(1+\delta^2)(p-1)^2}{(y_a-m)((y_a+q)^2+(p-1)^2)} + \frac{(1+\delta^2)(p+1)^2}{(d-y_a)((y_a-q)^2+(p+1)^2)}\right]\frac{\mathrm{d}y_a}{\mathrm{d}y}.$$

Since $\mathrm{d}y_a/\mathrm{d}y > 0$ and since $M < y < D$ is equivalent to $m < y_a < d$, $\mathrm{d}G/\mathrm{d}y = D^2F(y)/DF(y) > 0$ is satisfied, where $D^2F(y)$ denotes the second derivative of F. Since $DF(y)$ is negative for $M < y < D$, $D^2F(y)$ is also negative. ■

Then we obtain the following from theorems 3 and 4:

Theorem 5. *$F(I) \subseteq I$ and $|DF(y)| > 1$ on I are satisfied if*

$$DF(y_L) < -1. \tag{16}$$

Referring to Li *et al.* (1978), $|DF(y)| > 1$ for $F : I \to I$ guarantees that F is ergodic and has positive Lyapunov exponent, hence F exhibits chaos. Since y_L is given by $F(D_-)$ or $F^2(D)$ and since F and DF are given by analytic formula (9) and (12), respectively, the chaos generating condition (16) is described by three parameters (δ, p, q) or (a, b, c). This condition is satisfied in the shaded region in figure 7. Note that the condition (16) is 'sufficient' to chaos generation and we have observed various chaotic attractors without this condition. In figure 7, the curve l_c implies $y_L = M$ and almost attractors are to be chaotic under this curve. Also, the curve l_d in the shaded region implies $F^3(D) = F^2(D)$. Under this curve, the following is satisfied:

$$F^3(D) < F^2(D) < D. \tag{17}$$

If (17) is satisfied and if an orbit enters into $I_L \equiv [y_L, D)$ then it must hit I_L even times by it goes out of I_L hence two asymmetric single-screw attractors as figure 5*f* exist. The system exhibits symmetric double-screw attractor upper the curve l_d. That is, $F^3(D) = F^2(D)$ gives the boundary between double and single-screw chaos.

4. Conclusion

We have analysed chaos and fundamental bifurcations from a simple hysteresis chaos generator. Deriving one-dimensional return map rigorously, we give a sufficient condition for chaos generation and give fundamental bifurcation sets. Some of the theoretical results are verified by laboratory experiments. Roughly speaking, stretching by negative resistor and folding by hysteresis are basic for chaos generation form the circuit. Also hitting velocity ($\dot{x}$) at the threshold (Th_- or Th_+) changes the slope of the return map and causes periodic window. Then the constrained dynamics on two switched plane simplify the rigorous analysis. Now we are trying to develop the theoretical result into higher-dimensional cases. On the other hand (Hasler *et al.* 1993) has begun to apply our circuit to secure communication. We also try to apply the circuit for control of chaos, synchronization of chaos and related engineering systems.

PHILOSOPHICAL TRANSACTIONS OF THE ROYAL SOCIETY A MATHEMATICAL, PHYSICAL & ENGINEERING SCIENCES

Finally, we thank L. O. Chua, H. Kawakami, M. Hasler, W. Schwarz and K. Mitsubori for exciting discussions.

References

Chua, L. O., Komuro, M. & Matsumoto, T. 1986 The double scroll family. *IEEE Trans.* **CAS-33**, 1073–1118.

Chua, L. O., Wu, C. W., Huang, A. & Zhong, G.-Q. 1993 A universal circuit for studying and generating chaos. *IEEE Trans.* **CASI-40**, 732–761.

Hasler, M., Dedieu, H., Kennedy, M. P. & Schweizer, J. 1993 Secure communication system via Chua's circuit. In *Proc. NOLTA Workshops, Hawaii*, pp. 87–92.

Kennedy, M. P. & Chua, L. O. 1991 Hysteresis in electronic circuits: a circuit theorist's perspective. *Int. J. Circuit Theory Applic.* **19**, 471–515.

Li, T. Y. & Yorke, J. A. 1978 Ergodic transformations from an interval into itself. *Trans. Am. math. Soc.* **235**, 183–192.

Newcomb, R. & El-leithy, N. 1984 A binary hysteresis chaos generator. *Proc. IEEE/ISCAS*, pp. 856–859.

Ogorzałek, M. J. 1993 Taming chaos. II. Control. *IEEE Trans.* **CASI-40**, 700–706.

Ott, E. 1993 *Chaos in dynamical systems.* Cambridge University Press.

Ott, E., Grebogi, C. & Yorke, J. A. 1990 Controlling chaos. *Phys. Rev. Lett.* **64**, 1196–1199.

Pecora, L. M. & Carrol, T. L. 1990 Synchronization in chaotic systems. *Phys. Rev. Lett.* **64**, 821–824.

Saito, T. 1985 On a hysteresis chaos generator. *Proc. IEEE/ISCAS*, pp. 847–849.

Saito, T. 1990 An approach toward higher-dimensional hysteresis chaos generators. *IEEE Trans.* **CAS-37**, 399–409.

Saito, T. & Mitsubori, K. 1994 Hyperchaos and related phenomena from odd-dimensional hysteresis system. In *Nonlinear dynamics of electronic systems* (ed. A. C. Davies & W. Schwarz), pp. 294–311. World Scientific.

Suzuki, T. & Saito, T. 1994 On fundamental bifurcations from a hysteresis hyperchaos generator. *IEEE Trans.* **CASI-41**, 876–884.

PHILOSOPHICAL TRANSACTIONS OF THE ROYAL SOCIETY A MATHEMATICAL, PHYSICAL & ENGINEERING SCIENCES